PLANNED WIND TUNNEL EXPERIMENTS AT DLR KÖLN FOR THE REUSABILITY FLIGHT EXPERIMENT (REFEX)

Andreas K. Flock, Thomas Thiele, Dominik Neeb, Ali Gülhan

German Aerospace Center (DLR), Supersonic and Hypersonic Technologies Department
Linder Höhe, 51147 Köln, Germany

ABSTRACT

With the long term goal to investigate technologies for more affordable access to space, DLR is investigating a generic, reusable booster stage in its Reusability Flight Experiment (ReFEx). The present manuscript summarizes the planned wind tunnel experiments at DLR Cologne and gives additional information about the facilities. Over the course of the project, the following experiments are planned: First, static stability tests; second, dynamic stability tests; third, qualification tests for a Flush Air-Data Sensing (FADS) system; and fourth, aero-thermal tests. Finally, results for the static stability tests give insight into the static behavior of the vehicle at supersonic speeds. Furthermore, a pre-analysis of the FADS system revealed that the upstream influence of the canards onto the nose region is small.

Index Terms— Re-entry, Static Stability, Supersonic

1. INTRODUCTION

The German Aerospace Center (DLR) is investigating reusable launch vehicle concepts in several projects. One of them is the Reusability Flight Experiment, short ReFEx [1, 2, 3, 4, 5]. ReFEx is focused on flying a generic, winged booster stage on top of a sounding rocket experiment [6] and on actively guiding and controlling its trajectory [7, 8] to demonstrate re-usable technologies. The flight should demonstrate that the vehicle can pass the hypersonic, supersonic and transonic velocity range, down to a Mach number of 0.8, which defines the end of experiment. The flight vehicle is a generic winged booster stage with movable canards, a vertical stabilizer with rudder, and fixed delta wings (figure 1).

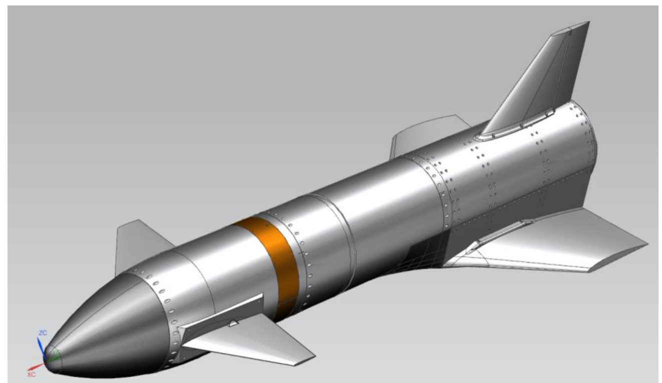

Fig. 1. CAD model of the ReFEx flight configuration; image from DLR-BT-RSI.

For the ascent phase, the payload is mounted on a VSB 30 sounding rocket, which is spin-stabilized. For a sufficient static margin and to avoid any large asymmetries near the rocket tip, the payload is covered by a fairing during ascent. To optimize the used space under the fairing cover, the wings are folded upwards. The vehicle is heavily instrumented with pressure, temperature, heat flux, and fiber optic sensors. Furthermore, optical and infrared cameras are installed [9].

The goal to perform a controlled flight from hypersonic to subsonic velocities imposes challenges during the aerodynamic design process. In addition, the flexibility during the design was limited, as the vehicle had to be placed on top of a non-controlled rocket. This resulted in two main phases during the aerodynamic flight: First, during re-entry at hypersonic Mach numbers and down to $M \approx 1.5$, the vehicle flies on its back, rolled by $\gamma = 180\,\text{deg}$. This is necessary to provide enough directional stability at large angles of attack. Second, at $M \approx 1.5$, the vehicle performs a roll-maneuver to reach its normal position, namely $\gamma = 0\,\text{deg}$. This is necessary to reach trimmable flight conditions at lower angles of attack and therefore better L/D. A detailed overview of the aerodynamic design, which was performed with CFD, is given in [10, 11].

The current manuscript presents the wind tunnel experiments that mainly serve two purposes. First, they are used to validate the CFD results and back-up the aerodynamic data base. Second, they are used to calibrate the FADS system and to study aero-thermal effects that occur at large Mach numbers. It is planned to perform four sets of wind tunnel tests. First, static stability tests with a six degree of freedom (6-DOF) forces and moments balance. Second, dynamic stability tests to measure damping properties during a rotary movement. Third, qualification tests for the FADS system, which is located near the nose of the vehicle. Fourth, aero-thermal tests to study aero-thermal heating at sensitive locations. In the following the planned tests are described in more detail, along with the used facilities and methodology. Next, current results are presented, which focus on the static stability tests and on a pre-analysis for the FADS system. Finally, the paper closes with a discussion of the results and an outlook.

2. PLANNED EXPERIMENTS

2.1. Static Stability Measurements

A scaled model of ReFEx was designed to fit into the TMK test section (figure 2). The limiting size parameter was a maximum blockage of 1% during tests within the transonic test section. This led to a scaling factor of 1 : 13, and a blockage of 1% at angle of attack of approximately 21 deg. During tests with the supersonic test section, angle of attack can be increased further, as blockage is less critical. The vehicle fuselage and wings formed the main body, to which additional modular components could be mounted (figure 3). Those were different canards for angles of 0 deg, ±5 deg, ±10 deg, and ±15 deg; and three different vertical stabilizers with varying rudder deflections of 0 deg, 5 deg, and 10 deg.

2.2. Dynamic Stability Measurements

In a subsequent wind tunnel study, the dynamic damping coefficients will be investigated. Two different techniques were previously used in our department, namely the forced and the free oscillation techniques [12, 13]. In both cases the model is mounted with a cross-flexure and rotates around the y-axis. Thus, only the longitudinal motion is investigated dynamically.

For the current project, the preparations for the dynamic measurements are still ongoing. At the moment, the feasibility of a cross flexure that allows for a roll oscillation is being investigated. No further results about the dynamic stability measurements are presented in this manuscript.

2.3. Flush Air-Data Sensing (FADS) System Measurements

The planned Flush Air-Data Sensing (FADS) system consists of several pressure ports in the nose region [9]. The sensors are located along the lines indicated by vertical and horizontal cut in figure 2, and should be in the circular section which lies at $x/L < 0.011$. With a numerical algorithm, the angle of attack α, angle of side slip β, the dynamic pressure q_∞, and static pressure p_∞ of the free stream can be calculated. These values include the direction and velocity of the relative wind, which is not considered in the on-board attitude and GPS systems. There are two options to set up the algorithm, which are currently under investigation. First, a so called triples algorithm can be used. This approach is valid for blunt bodies and needs to be calibrated to be valid over a broad range of Mach numbers [14]. Second, a table lookup, which was used in a previous flight experiment during for the post-processing analysis [15].

As both approaches require an aerodynamic database, a separate wind tunnel model will be built to serve this purpose. An essential question is imposed by the ReFEx design, namely: How much do the aerodynamic control surfaces, i.e. especially the canards, influence the upstream nose region that contains the pressure ports? We expect that the influence is larger for low Mach numbers, but generally we hope that there is a nose region which is unaffected by canard deflection. This would drastically reduce the FADS analysis and the scope of the aerodynamic database. The question above is examined in section 4.

2.4. Aero-Thermal Measurements

During its re-entry flight, ReFEx will reach low hypersonic Mach numbers, presumably up to Mach 5-6. Therefore, experiments are planned to investigate aero-thermal effects, such as surface heating. These will be performed in the hypersonic wind tunnel H2K (see section 3) and if necessary, the arc heated facilities L2K and L3K can be involved as well.

During the ReFEx flight, several instrumentation components measure surface temperature. For example, two infrared cameras at the front measure surface heating of the canards and several thermo couples and heat transfer gauges measure temperature and wall heat transfer at other locations. Therefore, during the tests in the wind tunnels, the transient heating behavior induced by the flow will be investigated to better understand these effects. If necessary, critical components or materials with surface coatings, can be tested in the arc heated facilities. No further results about the aero-thermal measurements are presented in this manuscript.

3. FACILITIES AND METHODOLOGY

3.1. Trisonic Wind Tunnel - TMK

For the stability measurements and the FADS system measurements the trisonic wind tunnel (TMK) is used [16]. TMK is a cold flow, blow down wind tunnel, that

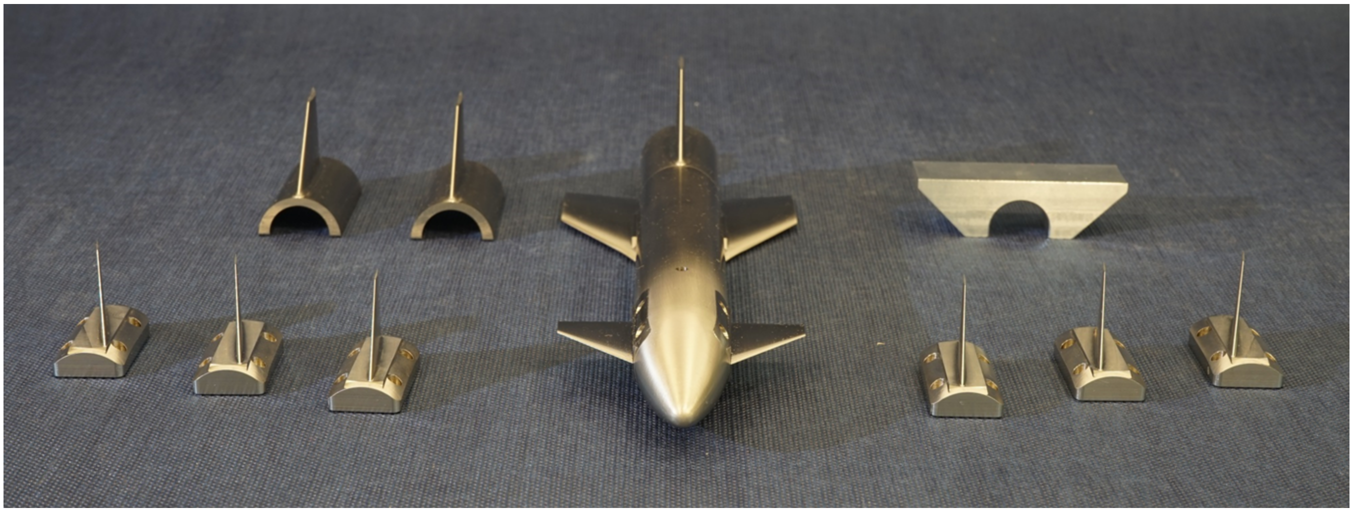

Fig. 2. ReFEx wind tunnel model for 6-DOF static forces and moments measurements in Transonic Facility (TMK).

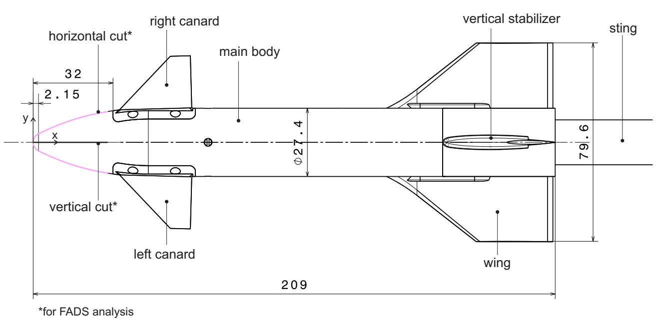

Fig. 3. Technical drawing of ReFEx wind tunnel model.

uses dried air from high pressure reservoirs for a controlled expansion through an adaptable Laval nozzle (see figure 4). The test section is rectangular and measures 0.6×0.6 m^2. Run times are on the order of $40 - 60$ s. Two different wind tunnel configurations exist: First, a transonic test section, that covers the Mach number range from 0.5 to 1.2. Second, a supersonic test section, that covers Mach numbers from 1.4 to 4.5. By using a heater system and an ejector, attached to the subsonic diffuser, the Mach and Reynolds number range can be further increased to higher and lower values, respectively (see figure 5). Thus, TMK covers a broad range of Mach and Reynolds numbers and allows for testing at low hypersonic, supersonic, tran- and subsonic velocities. This makes it a crucial facility for the scientific research throughout ReFEx.

3.2. Hypersonic Wind Tunnel - H2K

To extend the Mach numbers to larger values, and to investigate aero-thermal effects such as convective heat transfer due to skin friction, tests are also performed in the hypersonic wind tunnel facility (H2K) [17]. H2K is a blow-down wind tunnel that uses dried air from a high pressure reservoir (figure 6). This air is released through a Laval nozzle with circular exit (diameter 0.6 m). The test section is a free jet test section and air is released through a diffuser into a vacuum sphere. Run times are on the order of 30 s. Five different Laval nozzles exist for Mach numbers of 5.3, 6, 7, 8.7, and 11.2. By setting the accessed pressure of the high pressure reservoir, and by adjusting the electrical heater, Reynolds number can be varied in a broad range (figure 7).

3.3. Six-degree-of-freedom (6-DOF) Balance System

As results for the static stability measurements are shown in this manuscript, the main measurement device, namely a six-degree-of-freedom balance, is explained in the following. A 3/4 inch forces and moment balance from the TASK corporation was used (figure 8). The balance main axis is aligned with the ReFEx wind tunnel model and mounted onto a sting. With the balance system and a calibration, the forces and moments in all three directions can be measured.

4. CURRENT RESULTS

4.1. Static Stability Measurements

A first test campaign with the ReFEx wind tunnel model (figure 2) was performed during summer 2019. During the tests, the angle of attack of the model was varied and various information was collected. Figure 9, for example, shows Schlieren images during wind tunnel runs for the Mach numbers of 2.5 (left) and 4.5 (right), and at an angle of attack of 0 deg. The canards are deflected to

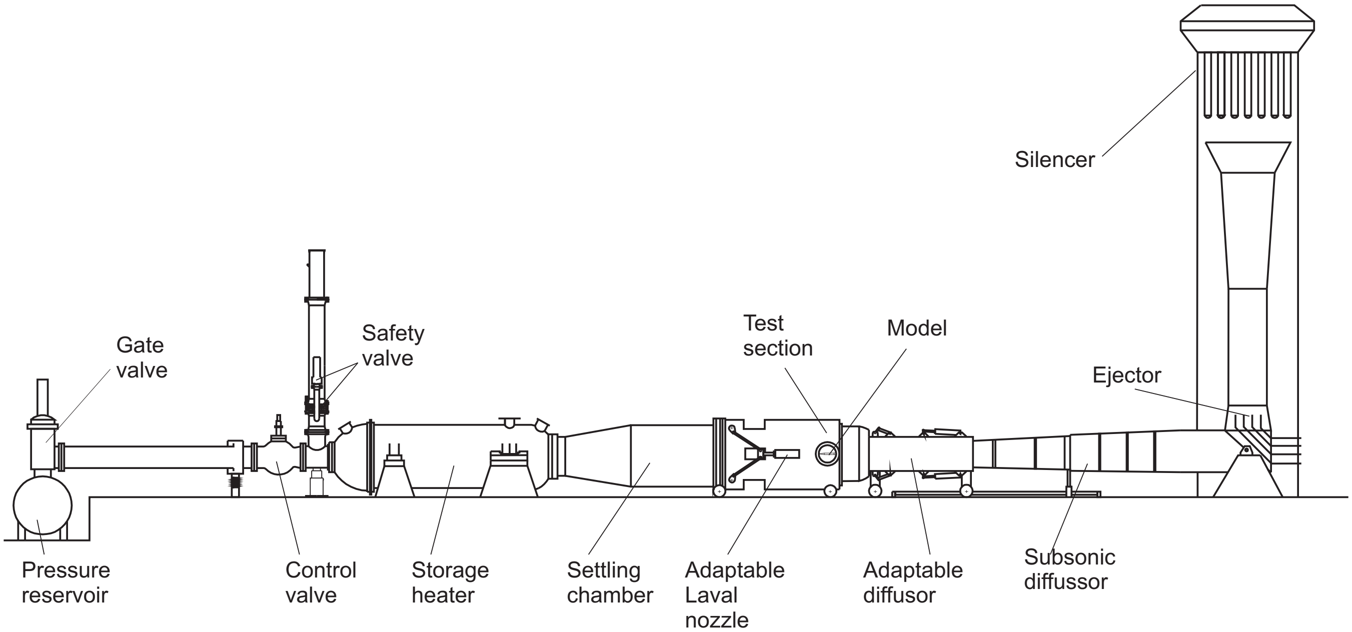

Fig. 4. Schematic diagram of Trisonic Wind Tunnel Facility (TMK) at DLR Köln.

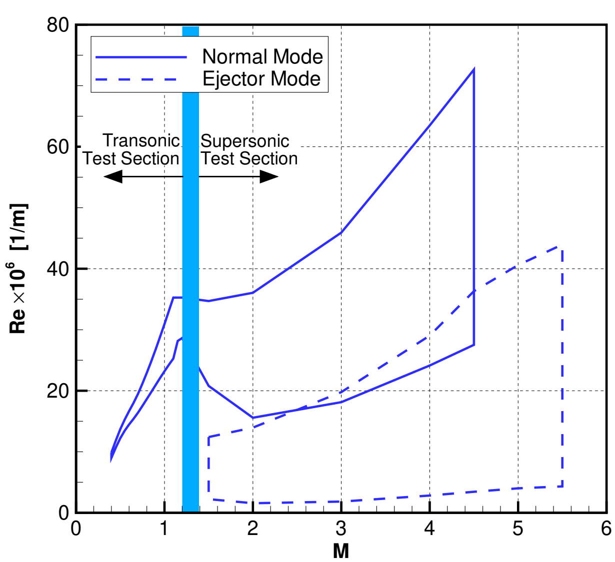

Fig. 5. Mach and Reynolds number range of TMK.

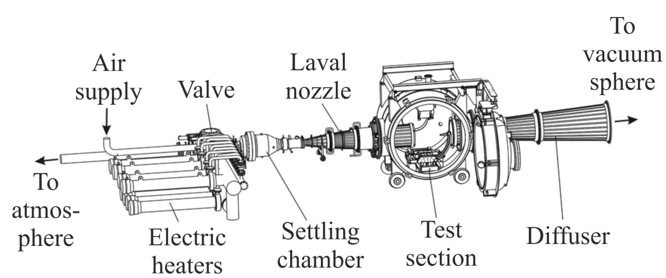

Fig. 6. Schematic diagram of hypersonic wind tunnel facility (H2K) at DLR Köln.

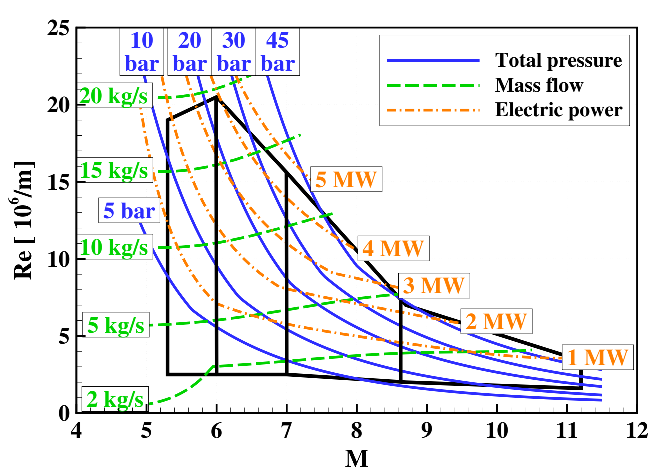

Fig. 7. Mach and Reynolds number range of H2K.

Fig. 8. 3/4 inch TASK balance.

-5 deg and therefore the shocks towards downside of the model are stronger.

Figure 10 shows the Schlieren shock structure for an angle of attack of 28 deg. For the low Mach number case, the bow shock encloses the entire geometry. In contrast, for the higher Mach number case, the bow shock intersects with the vertical stabilizer. On the lee-side there are several shock structures caused by various components of the model, such as the leading and trailing edges of the canards or the wings. On the windward side for the Mach 2.5 case, the shock structure is dominated by the interaction of the bow shock and trailing edge shock of the canards; for the Mach 4.5 case, the shock layer is very narrow and no additional features are detectable.

Figure 11 shows the pitching moment coefficients for different canard deflections at a moment reference location $57\% \times L$ downstream of the nose. The angle of attack was lowered from 0 deg to -40 deg and again increased to 0 deg. As practically no difference between the pitching-down and pitching-up movement was detectable, the rate of change of angle of attack was considered to be low enough to produce quasi-steady results. For the low Mach number, the slope of the pitching moment coefficient is negative for $\alpha < -5$ deg. For the large Mach number, the slope of the pitching moment coefficient becomes positive at $\alpha \approx -20$ deg, $\alpha \approx -18$ deg, and $\alpha \approx -16$ deg, for canard deflections of $\eta_{\mathrm{L,R}} = -15$ deg, -10 deg, and -5 deg, respectively. The investigated canards allow for trimming, that is $CMY = 0$, between $-38\,\mathrm{deg} < \alpha_{\mathrm{trim}} < -31\,\mathrm{deg}$ for Mach 2.5. This range slightly increases to $-40\,\mathrm{deg} < \alpha_{\mathrm{trim}} < -30\,\mathrm{deg}$ for Mach 4.5. All trim conditions are statically stable.

4.2. FADS System

To investigate the upstream influence of the canards, Computational Fluid Dynamics (CFD) calculations were performed for the canard angles -10 deg, 0 deg, and $+10$ deg. Cross sectional views for $z = 0$ (horizontal cut) and $y = 0$ (vertical cut) are shown in figure 12 for angles of attack of $\alpha = -25$ deg, 0 deg, and $+25$ deg and for Mach 2.

Except for small fluctuations due to slightly varying meshes, the pressure coefficients c_p are practically identical for different canard angles. This indicates that there is no upstream propagation from the canard section.

Figure 13 shows the same cross sectional plots, but for subsonic flight at the end of experiment condition ($M = 0.8$). The orange ellipses indicate an upstream influence of the canards. In general there is an unaffected region near the nose, and increasing deviations further downstream. In the horizontal cut, the deviations are symmetrical and become negligible for $x/L < 0.025$; in the vertical plane, the deviations are asymmetrical (dashed vs. solid ellipse in figure 13) and become negligible for $x/L < 0.015$.

5. OUTLOOK

Future work is focused on the topics described in section 2. As of now, the static stability measurements are being evaluated and processed. In a next step they will be validated with the CFD results. Furthermore, the remaining wind tunnel campaigns are being prepared.

6. REFERENCES

[1] Peter Rickmers, Waldemar Bauer, Martin Sippel, and Sven Stappert, "Refex: Reusability flight experiment a flight experiment to demonstrate controlled aerodynamic flight from hypersonic to subsonic velocities with a winged rlv," in 7th European Conference for Aeronautics and Space Sciences (EUCASS), 2017.

[2] Waldemar Bauer, Peter Rickmers, Alexander Kallenbach, Sven Stappert, René Schwarz, Marco Sagliano, Janis S. Häseker, Andreas K. Flock, Thomas Thiele, Andreas Bierig, Jens Windelberg, and Eugen Ksenik, "Upcoming dlr reusability flight experiment," in 68th International Astronautical Congress, 2017, number IAC-17-D2.6.1.

[3] Peter Rickmers, Waldemar Bauer, Martin Sippel, Sven Stappert, René Schwarz, Marco Sagliano, Guilherme Fragoso Trigo, Guido Wübbels, and Hauke Martens, "An update of the upcoming dlr reusability flight experiment - refex," in 69th International Astronautical Congress (IAC), 2018, number IAC-18.D2.6.1.

[4] Peter Rickmers, Waldemar Bauer, Sven Stappert, Daniel Kiehn, and Martin Sippel, "Current status of the dlr reusability flight experiment - refex," in HiSST: International Conference on High-Speed Vehicle Science Technology, 2018.

[5] Peter Rickmers, Waldemar Bauer, Guido Wübbels, and Sebastian Kottmeier, "Refex: Reusability flight experiment - a project overview," in 8th European Conference for Aeronautics and Space Sciences (EUCASS), 2019.

Fig. 9. Schlieren images of the ReFEx model during a Mach 2.5 (left) and Mach 4.5 (right) run; $\eta_{\mathrm{L,R}} = -5\,\mathrm{deg}$, $\alpha = 0\,\mathrm{deg}$.

Fig. 10. Schlieren images of the ReFEx model during a Mach 2.5 (left) and Mach 4.5 (right) run; $\eta_{\mathrm{L,R}} = -5\,\mathrm{deg}$, $\alpha = 28\,\mathrm{deg}$.

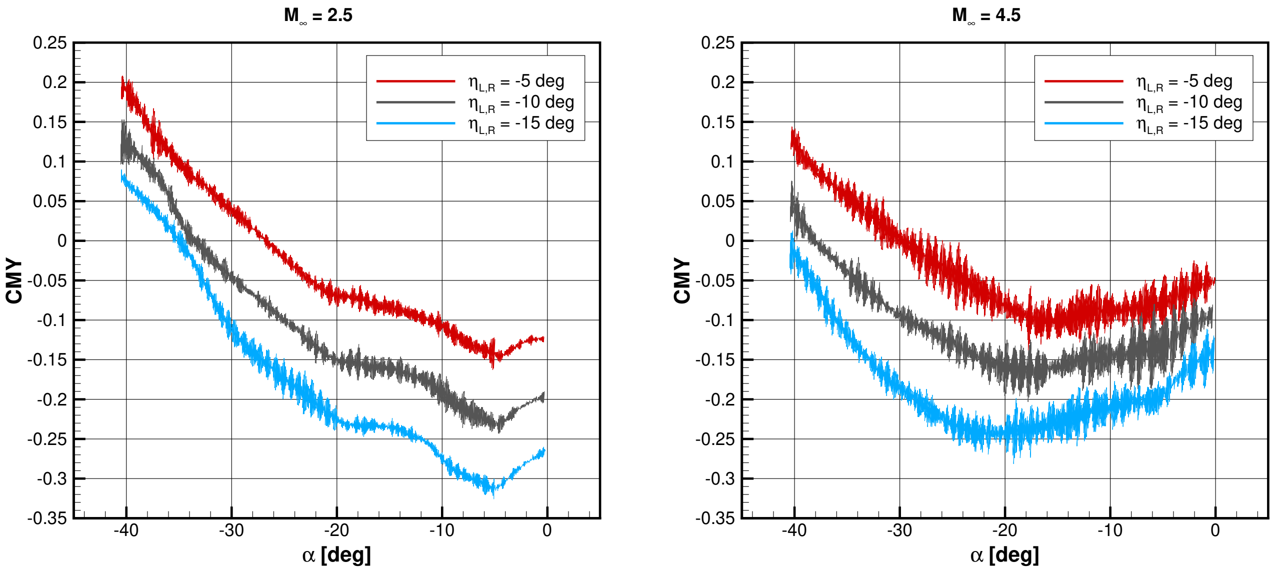

Fig. 11. Pitching moment coefficient for different canard deflections and Mach numbers.

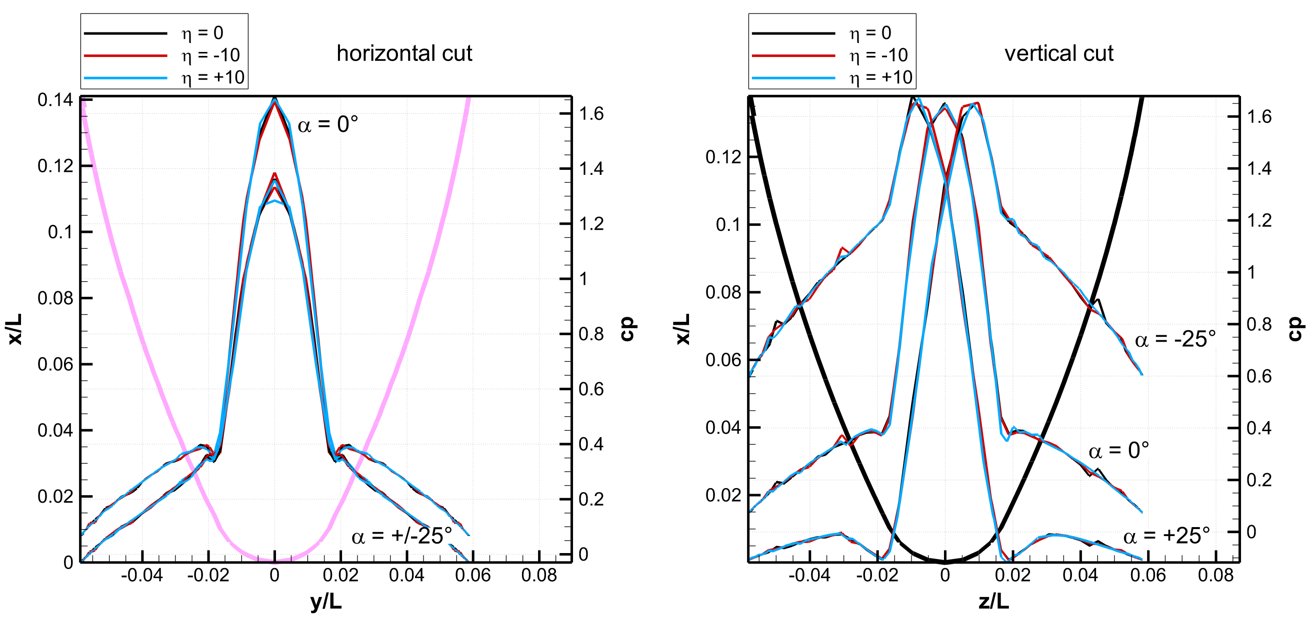

Fig. 12. Cross sectional views of pressure coefficient in the nose region for Mach 2; cuts as sketched in figure 2.

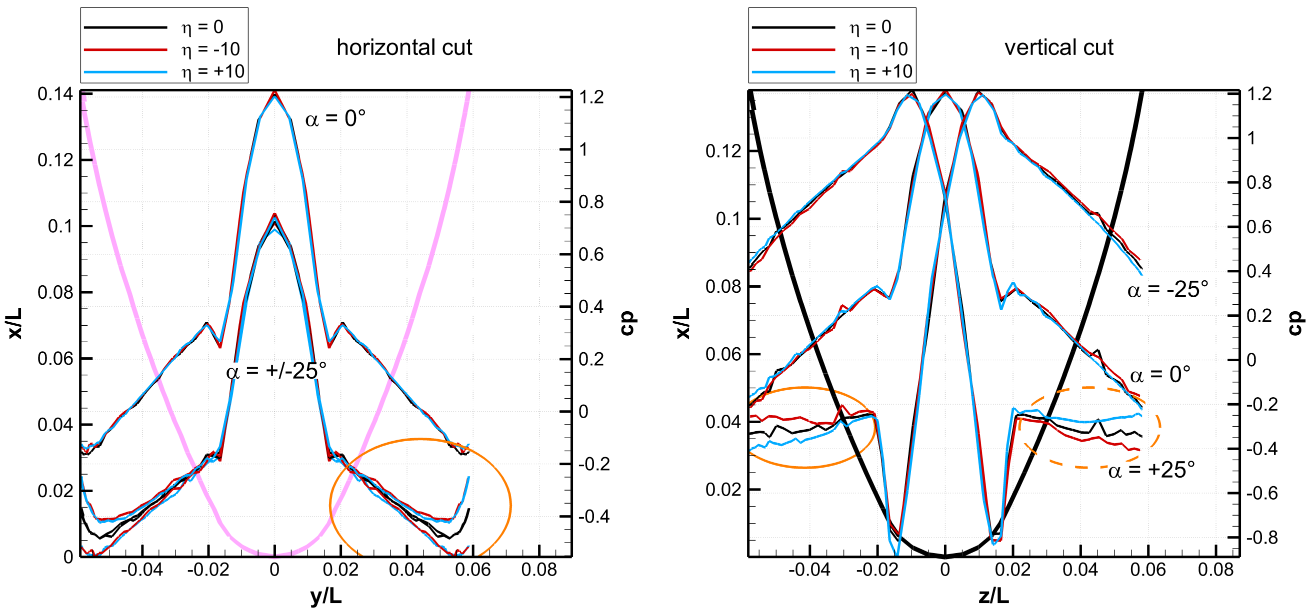

Fig. 13. Cross sectional views of pressure coefficient in the nose region for Mach 0.8; cuts as sketched in figure 2.

[6] Rainer Kirchhartz, Alexander Schmidt, Marcus Hörschgen-Eggers, and Alexander Kallenbach, "Refex launch with a sounding rocket - a challenging mission on a reliable carrier," in 8th European Conference for Aeronautics and Space Sciences (EUCASS), 2019.

[7] René Schwarz, Daniel Kiehn, Guilherme F. Trigo, Bronislovas Razgus, Andreas Wenzel, David Seelbinder, Jan Sommer, Stephan Theil, Markus Markgraf, Michael Dumke, Martin Reigenborn, Matias Bestard Köner, Marco Solari, Benjamin Braun, and Dennis Pfau, "Overview of flight guidance, navigation, and control for the dlr reusability flight experiment (refex)," in 8th European Conference for Aeronautics and Space Sciences (EUCASS), 2019.

[8] Sven Stappert, Peter Rickmers, Waldemar Bauer, and Martin Sippel, "Mission analysis and preliminary re-entry trajectory desig of the dlr reusability flight experiment refex," in 8th European Conference for Aeronautics and Space Sciences (EUCASS), 2019.

[9] Thomas Thiele, Frank Siebe, Andreas K. Flock, and Ali Gülhan, "Flight instrumentation for the reusability flight experiment refex," in 8th European Conference for Aeronautics and Space Sciences (EUCASS), 2019.

[10] Clemens Merrem, Viola Wartemann, and Thino Eggers, "Preliminary aerodyanmic design of a reusable booster flight experiment," in HiSST: International Conference on High-Speed Vehilce Science Technology, 2018.

[11] Clemens Merrem, Daniel Kiehn, Viola Wartemann, and Thino Eggers, "Aerodynamic design of a reusable booster stage flight experiment," in 8th European Conference for Aeronautics and Space Sciences (EUCASS), 2019.

[12] Ali Gülhan, Frank Siebe, Thomas Thiele, Dominik Neeb, John Turner, and Josef Ettl, "Sharp Edge Flight Experiment-II Instrumentation Challenges and Selected Flight Data," Journal of Spacecraft and Rockets, vol. 51, no. 1, pp. 175–186, 2014.

[13] Thomas Gawehn and Ali Gülhan, "Experimental study on static and dynamic stability of a blunt body configuration," in International Conference on Flight Vehicles, Aerothermodynamics and Re-entry Missions & Engineering, 2019.

[14] Stephen A. Whitmore, Brent R. Cobleigh, and Edward A. Haering, "Design and calibration of the x-33 flush airdata sensing (fads) system," Tech. Rep. NASA/TM-1998-206540, NASA, 1998.

[15] Thomas Thiele, Dominik Neeb, and Ali Gülhan, "Post-flight hypersonic ground experiments and fads flight data evaluation for the shefex-ii configuration," in Proceedings of the 8th European Symposium on Aerothermodynamics for Space Vehicles, 2015.

[16] Helmut Esch, “The 0.6 x 0.6m tri-sonic wind tunnel (tmk) of the dfvlr in köln-porz (german),” Internal Report 86-21, Deutsche Forschungs- und Versuchsanstalt für Luft- und Raumfahrt, 1986.

[17] Franz-Joachim Niezgoda, “Der Hyperschallwindkanal H2K des DLR in Köln-Porz,” Tech. Rep. 2001-01, Deutsches Zentrum für Luft- und Raumfahrt, Cologne, 2001.